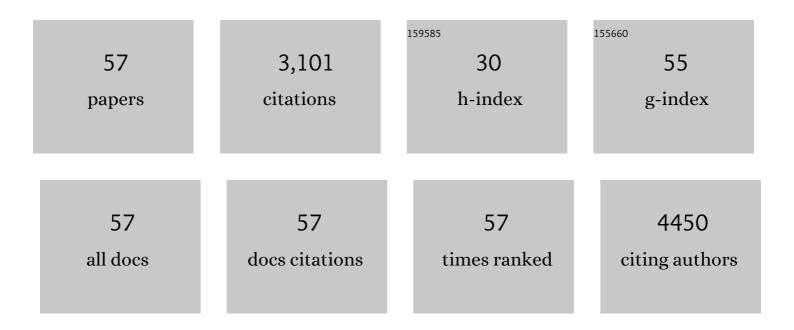
Xiaotong Jiang

List of Publications by Year in descending order

Source: https://exaly.com/author-pdf/4288912/publications.pdf Version: 2024-02-01



#	Article	IF	CITATIONS
1	The production and characteristics of solid lipid nanoparticles (SLNs). Biomaterials, 2003, 24, 1781-1785.	11.4	352
2	Comparison of dye degradation efficiency using ZnO powders with various size scales. Journal of Hazardous Materials, 2007, 141, 645-652.	12.4	339
3	Preparation and gas-sensing properties of Ce-doped ZnO thin-film sensors by dip-coating. Materials Science and Engineering B: Solid-State Materials for Advanced Technology, 2007, 137, 53-58.	3.5	229
4	Specific role of polysorbate 80 coating on the targeting of nanoparticles to the brain. Biomaterials, 2004, 25, 3065-3071.	11.4	181
5	A comparative study on UV light activated porous TiO2 and ZnO film sensors for gas sensing at room temperature. Ceramics International, 2012, 38, 503-509.	4.8	134
6	Fabrication and formaldehyde gas-sensing property of ZnO–MnO2 coplanar gas sensor arrays. Sensors and Actuators B: Chemical, 2010, 145, 457-463.	7.8	122
7	Identification and pattern recognition analysis of Chinese liquors by doped nano ZnO gas sensor array. Sensors and Actuators B: Chemical, 2005, 110, 370-376.	7.8	109
8	Selectively enhanced UV and NIR photoluminescence from a degenerate ZnO nanorod array film. Journal of Materials Chemistry C, 2014, 2, 4566.	5.5	104
9	Characterization of Chinese vinegars by electronic nose. Sensors and Actuators B: Chemical, 2006, 119, 538-546.	7.8	99
10	Corrosion characteristics of copper microparticles and copper nanoparticles in distilled water. Corrosion Science, 2006, 48, 3924-3932.	6.6	86
11	Preparation, structure and thermal stability of Cu/LDPE nanocomposites. Materials Chemistry and Physics, 2006, 95, 122-129.	4.0	82
12	Comparison on photocatalytic degradation of gaseous formaldehyde by TiO2, ZnO and their composite. Ceramics International, 2012, 38, 4437-4444.	4.8	73
13	â€~Sensory analysis' of Chinese vinegars using an electronic nose. Sensors and Actuators B: Chemical, 2008, 128, 586-593.	7.8	59
14	The effects of oxygen partial pressure on the microstructures and photocatalytic property of ZnO nanoparticles. Physica E: Low-Dimensional Systems and Nanostructures, 2008, 40, 2724-2729.	2.7	57
15	Full mineralization of toluene by photocatalytic degradation with porous TiO2/SiC nanocomposite film. Journal of Alloys and Compounds, 2013, 552, 504-510.	5.5	55
16	An entire feature extraction method of metal oxide gas sensors. Sensors and Actuators B: Chemical, 2008, 132, 81-89.	7.8	52
17	Enhancement of photocatalytic property of ZnO for gaseous formaldehyde degradation by modifying morphology and crystal defect. Journal of Alloys and Compounds, 2013, 550, 190-197.	5.5	51
18	Improvement of gaseous pollutant photocatalysis with WO3/TiO2 heterojunctional-electrical layered system. Journal of Hazardous Materials, 2011, 196, 52-58.	12.4	49

XIAOTONG JIANG

#	Article	IF	CITATIONS
19	Formaldehydeâ€, Benzeneâ€, and Xyleneâ€Sensing Characterizations of Zn–W–O Nanocomposite Ceramics. Journal of the American Ceramic Society, 2007, 90, 3263-3267.	3.8	46
20	Controlled organization of ZnO building blocks into complex nanostructures. Journal of Colloid and Interface Science, 2006, 297, 570-577.	9.4	45
21	Porous LaFeO3/SnO2 nanocomposite film for CO2 detection with high sensitivity. Materials Chemistry and Physics, 2017, 186, 228-236.	4.0	45
22	Formaldehyde sensor based on Ni-doped tetrapod-shaped ZnO nanopowder induced by external magnetic field. Physica E: Low-Dimensional Systems and Nanostructures, 2008, 41, 235-239.	2.7	41
23	Synthesis, formation mechanism and sensing properties of WO3 hydrate nanowire netted-spheres. Materials Research Bulletin, 2010, 45, 1541-1547.	5.2	41
24	Synthesis, formation mechanism and illuminated sensing properties of 3D WO3 nanowall. Journal of Alloys and Compounds, 2010, 495, 88-92.	5.5	41
25	Non-isothermal crystallization behavior of low-density polyethylene/copper nanocomposites. Thermochimica Acta, 2005, 427, 129-135.	2.7	40
26	Spoiling and formaldehyde-containing detections in octopus with an E-nose. Food Chemistry, 2009, 113, 1346-1350.	8.2	38
27	Synthesis and characterization of ZnO nanostructures by two-step oxidation of Zn nano- and microparticles. Journal of Crystal Growth, 2006, 289, 663-669.	1.5	33
28	Comparative study of ZnO nanorod array and nanoparticle film in photoelectric response and charge storage. Journal of Alloys and Compounds, 2014, 585, 267-276.	5.5	33
29	Preparation and photocatalytic activity of TiO2/CeO2/Bi2O3 composite for Rhodamine B degradation under visible light irradiation. Journal of Alloys and Compounds, 2013, 581, 385-391.	5.5	31
30	Highly photoactive sensor based on NiO modified TiO2 porous film for diethyl ether. Sensors and Actuators B: Chemical, 2014, 195, 439-445.	7.8	31
31	An efficient method to modulate the structure, morphology and properties of WO3 through niobium doping. Journal of Alloys and Compounds, 2014, 610, 132-137.	5.5	30
32	Characterization of Incidental Photon-to-electron Conversion Efficiency (IPCE) of porous TiO2/SnO2 composite film. Journal of Alloys and Compounds, 2013, 569, 88-94.	5.5	29
33	A novel method in the gas identification by using WO3 gas sensor based on the temperature-programmed technique. Sensors and Actuators B: Chemical, 2015, 206, 220-229.	7.8	29
34	Novel 1–3 metal nanoparticle/polymer composites induced by hybrid external fields. Composites Science and Technology, 2006, 66, 1558-1563.	7.8	25
35	A comparative study of microstructures on the photoelectric properties of tungsten trioxide films with plate-like arrays. Applied Surface Science, 2014, 297, 116-124.	6.1	23
36	Nanostructural ZnO based coplanar gas sensor arrays from the injection of metal chloride solutions: Device processing, gas-sensing properties and selectivity in liquors applications. Sensors and Actuators B: Chemical, 2011, 153, 415-420.	7.8	22

XIAOTONG JIANG

#	Article	IF	CITATIONS
37	A method for modeling and deciphering the persistent photoconductance and long-term charge storage of ZnO nanorod arrays. Nano Research, 2016, 9, 2972-3002.	10.4	21
38	Effect of the loading and size of copper particles on the mechanical properties of novel Cu/LDPE composites for use in intrauterine devices. Materials Science & Engineering A: Structural Materials: Properties, Microstructure and Processing, 2006, 429, 329-333.	5.6	20
39	Chitosan/alginate multilayer film for controlled release of IDM on Cu/LDPE composite intrauterine devices. Colloids and Surfaces B: Biointerfaces, 2013, 109, 82-89.	5.0	19
40	Tin oxide thick film by doping rare earth for detecting traces of CO2: Operating in oxygen-free atmosphere. Materials Research Bulletin, 2014, 52, 56-64.	5.2	19
41	Zn2+ release behavior and surface characteristics of Zn/LDPE nanocomposites and ZnO/LDPE nanocomposites in simulated uterine solution. Journal of Materials Science: Materials in Medicine, 2008, 19, 3319-3326.	3.6	17
42	Cupric ion release controlled by copper/low-density polyethylene nanocomposite in simulated uterine solution. Journal of Biomedical Materials Research - Part B Applied Biomaterials, 2007, 80B, 220-225.	3.4	16
43	Water absorption characteristics of novel Cu/LDPE nanocomposite for use in intrauterine devices. Journal of Biomedical Materials Research - Part B Applied Biomaterials, 2006, 79B, 345-352.	3.4	13
44	An alternate method of hierarchical classification for E-nose: Combined Fisher discriminant analysis and modified Sammon mapping. Sensors and Actuators B: Chemical, 2007, 127, 399-405.	7.8	13
45	Conduction model of coupled domination by bias and neck for porous films as gas sensor. Sensors and Actuators B: Chemical, 2013, 176, 217-224.	7.8	12
46	Applied low bias with high frequency for enhancing mineralization ability of WO3 as visible-light-driven photocatalyst in gas phase. Catalysis Communications, 2011, 16, 180-183.	3.3	11
47	Quantitative characterization of the long-term charge storage of a ZnO-based nanorod array film through persistent photoconductance. RSC Advances, 2018, 8, 16455-16463.	3.6	11
48	Electrochemical behaviour of copper/LDPE composites in the simulated uterine solution. Electrochimica Acta, 2006, 51, 5606-5611.	5.2	10
49	A novel simplified method for preparing ZnO nanoneedles via H2O2 pre-oxidation. Materials Chemistry and Physics, 2005, 93, 539-543.	4.0	9
50	Laser grooving of Al2O3 plate by a pulsed Nd:YAG laser: Characteristics and application to the manufacture of gas sensors array heater. Materials Science & Engineering A: Structural Materials: Properties, Microstructure and Processing, 2006, 435-436, 418-424.	5.6	9
51	A reaction model of metal oxide gas sensors and a recognition method by pattern matching. Sensors and Actuators B: Chemical, 2009, 135, 552-559.	7.8	9
52	IDM release behavior and surface characteristics of the novel Cu/IDM/LDPE nanocomposite for intrauterine device. Colloids and Surfaces B: Biointerfaces, 2009, 69, 276-280.	5.0	9
53	Temperature―and Atmosphereâ€Ðependent Defect Chemistry Model of <scp><scp>SnO</scp></scp> ₂ Nanocrystalline Film. Journal of the American Ceramic Society, 2014, 97, 2091-2098.	3.8	9
54	Microwave sintering of ZnO nanopowders and characterization for gas sensing. Materials Science and Engineering B: Solid-State Materials for Advanced Technology, 2011, 176, 181-186.	3.5	7

#	Article	IF	CITATIONS
55	Assessing multi-variable coupling effects of UV illumination, heat and oxygen on porous ZnO nanocrystalline film through electron concentration and mobility extraction. Physical Chemistry Chemical Physics, 2015, 17, 18045-18054.	2.8	6
56	Extraordinarily enhanced gas phase photoelectric response of CdS/TiO2 nanocomposite photoelectrode: CdS as a sensitizer and a hole capturer. Journal of Nanoparticle Research, 2013, 15, 1.	1.9	3
57	Electrochemical study of the corrosion behaviour of copper/low-density polyethylene microcomposite in the simulated uterine solution. Journal of Electroanalytical Chemistry, 2007, 603, 219-226.	3.8	2